Magnetic nanostructures for the manipulation of individual nanoscale particles in liquid environments (invited)

P. Vavassori, M. Gobbi, M. Donolato, M. Cantoni, R. Bertacco et al.

Additional information on J. Appl. Phys.

Magnetic nanostructures for the manipulation of individual nanoscale particles in liquid environments (invited)

P. Vavassori,[1,2] M. Gobbi,[1] M. Donolato,[3] M. Cantoni,[3] R. Bertacco,[3] V. Metlushko,[4] and B. Ilic[5]

[1]*CIC NanoGUNE Consolider, Donostia-San Sebastian 20018, Spain*
[2]*CNR-INFM S3, CNISM and Dipartimento di Fisica, Università di Ferrara, 44100 Ferrara, Italy*
[3]*Dipartimento di Fisica Politecnico di Milano, LNESS, Via Anzani 42, 22100 Como, Italy*
[4]*Department of Electrical and Computer Engineering, University of Illinois at Chicago, Chicago, Illinois 60607, USA*
[5]*Cornell Nanofabrication Facility, Cornell University, Ithaca, New York 14853, USA*

The manipulation of geometrically constrained magnetic domain walls (DWs) in nanoscale magnetic strips attracted much interest recently, with proposals for prospective memory and logic devices. Here we demonstrate that the high controllability of the motion of geometrically constrained DWs allows for the manipulation of individual nanoparticles in solution on a chip with the active control of position at the nanometer scale. Our approach exploits the fact that magnetic nanoparticles in suspension can be captured by a DW, whose position can be manipulated with nanometer scale accuracy in specifically designed magnetic nanowire structures. We hereby show that the precise control over DW nucleation, displacement, and annihilation processes in such nanostructures allows for the capture, transport, and release of magnetic nanoparticles. As magnetic nanoparticles with functionalized surfaces are widely used as molecule carriers or labels for single molecule studies, cell manipulation, and biomagnetic sensing, the accurate control over the handling of the single magnetic nanoparticle in suspension is a crucial building block for several applications in biotechnology, nanochemistry, and nanomedicine. © *2010 American Institute of Physics*. [doi:10.1063/1.3352579]

In perspective, the easy integration on chip of nanotransport lines and sensors of domain walls (DW) and particles will allow for the realization of complete functional devices for molecular manipulation, analysis, and synthesis, with continuous remote control of process. In nanoscale ferromagnetic wires (nanowires), shape anisotropy restricts the magnetization to lie parallel to the wire axis. In such a nanowire, a DW is a mobile interface, which separates regions of oppositely aligned magnetization. Each magnetic domain, has a head (positive or north pole) and a tail (negative or south pole). The resulting DWs are therefore either head-to-head (HH) or tail-to-tail (TT), and successive DWs along the nanowire alternate between HH and TT configurations. The motion of such geometrically confined DWs in nanoscale magnetic strips has recently become the focus of widespread theoretical[1,2] and experimental[3–7] research. Due to the geometrical confinement, the spin structure of a DW can be controlled via the lateral dimensions and film thickness of the nanowire, while the DW size is in the tens of nanometers range and hence such a DW can be manipulated as a "spin block" that have particlelike properties. Almost all the interest in this subject is hereby driven by the fact that DWs can be easily injected in a magnetic nanowire, manipulated and displaced between artificial pinning sites (notches, protrusions, corners, etc.) using magnetic fields or spin polarized currents,[8–10] as well as by the goal of understanding the DW dynamics itself. These aspects are also related to the potential for recently demonstrated technological application schemes that include magnetic random access memory[3] and logic devices.[11]

Submicrometer planar strips (planar nanowires) made from a soft magnetic material such as Permalloy (Py, $Ni_{80}Fe_{20}$) have been shown to form excellent conduits for DWs that can be nucleated and manipulated in a highly controllable way.[3–7] In addition it has been shown that, under the action of an externally applied magnetic field, DWs can be propagated through complex 2D and 3D networks of nanowires that contain bifurcation and intersection points.[11]

Besides these more traditional applications in the field of data storage technologies, in this communication, another potential application that exploits the manipulation of geometrically constrained magnetic DW in nanoscale magnetic strips is presented. In particular we show how magnetic particles in solution are moved and positioned with nanometer precision by means of a remote and low strength magnetic field that generates precisely predefined DW movements in a DW conduit structure. As magnetic nanoparticles are widely used for tagging molecules or cells, our method can be used for biological applications involving manipulation, transport, and sorting of molecules and cells on surfaces. Although this application of nanomagnetism to the fields of biotechnological and medical applications is still in its infancy, it already reveals its huge potential as one example of the synergetic combination of nanophysics, nanochemistry, and nanobiotechnology.
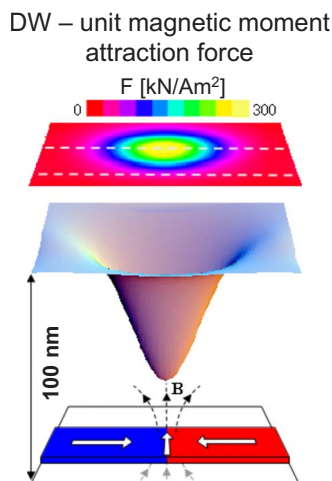
DW – unit magnetic moment attraction force

FIG. 1. (Color online) Color intensity plot of the modulus of the attractive force per unit magnetic moment, together with a sketch the potential energy surface, experienced by a point superparamagnetic with a unit magnetic moment placed on a plane at 100 nm from the upper surface of a "transverse" head-to-head DW nucleated in a conduit.
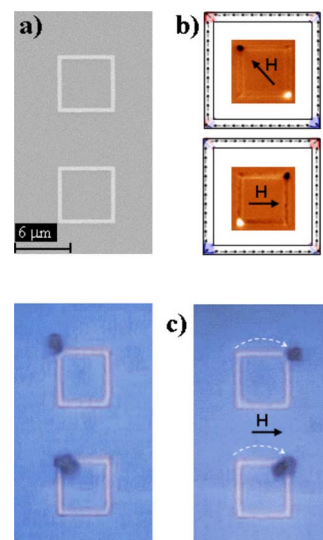

FIG. 2. (Color online) (a) SEM image of the Py square rings used in the experiment. (b) Micromagnetic simulations and MFM images showing the nucleation and the displacement of head-to-head and tail-to-tail DWs in a square ring. (c) optical microscopy images of the digital displacement of magnetic particles captured by the two DWs by applying an horizontal field of 150 Oe.

In the last years other techniques have been developed for the micromanipulation of magnetic particles as, e.g., microfabricated current carrying wires,[12] micromagnets,[13] and magnetic tweezers.[14] More recently, arrays of thin film magnetic elements were also proposed for the transport of single magnetic particles exploiting the stray field generated by the magnetization of the elements and the manipulation of each element magnetization using an external magnetic field.[15,16] However, none of these techniques achieved the true single particle manipulation ability at the nanoscale provided by the approach described here.

The basic ingredient of the application described here is the highly inhomogeneous magnetic stray field generated by a DW, of up to several kOe, which can trap a magnetic particle. This stray field is spatially localized at the nanometer scale due to the very confined geometric structure of the DW. The gradient of the magnetic stray field generated by the DW results in an attractive force, which tends to capture any magnetic nanoparticle that is moving in proximity of the DW location, as we previously ascertained in the case of DWs in Py square rings.[18]

Figure 1 shows a color intensity plot of the modulus of the attractive force, together with a sketch of the potential energy surface, experienced by a point superparamagnetic with a unit magnetic moment placed on a plane at 100 nm from the upper surface of a DW conduit structure in which a "transverse" HH DW has been nucleated. The plots have been calculated by computing, with the OOMMF public simulation platform,[17] the magnetic field $\mathbf{H}$ created in the surrounding space by the HH DW and using the following vector expression for the force: $\mathbf{F} = \mu_0(\mu \bullet \nabla)\mathbf{H}$, where μ is a unit magnetic moment ($\mu = 1$ Am^2) placed in a plane at 100 nm from the nanowire surface. As an example, a typical value of μ of commercially available superparamagnetic nanoparticles is of the order of $10^{-16} - 10^{-15}$ Am^2, in which case the intensity of the attractive force can be estimated to be in the 10–100 pN range in a plane 100 nm above the conduit.

The use of the DW stray field for trapping nano- and micron-sized superparamagnetic particles has been demonstrated experimentally in various cases: HH and TT DWs in Py nanorings[18] and DWs in thin garnet films.[19,20] In the latter case, it was shown that a DW in a garnet thin film can be used to drag and manipulate magnetic colloidal particles at a solid or fluid interface, however, with a limited control over the number of particles, the distance, and the direction.

The much higher control on the nucleation, displacement, and annihilation of DWs via external fields achievable in planar nanowires made from a soft magnetic material, induced us to explore the use of such structures as DW conduits to achieve a true nanometric manipulation of individual magnetic nanoparticles in wet environments. Additionally, the use of planar nanowires as DW conduits is particularly interesting since it may, in the future, make it possible to move DWs via spin polarized current pulses.[8–10]

In order to demonstrate the viability of the method, we first used square rings of Py, as the DWs motion in these structures is particularly simple and has been extensively investigated in previous articles.[21] The panel (a) of Fig. 2 shows the scanning electron microscopy (SEM) image of one type of structures used in the present experiment. They are 30 nm thick Py square rings with outside size of 6 μm and width of each segment of 200 nm, e-beam lithographically patterned on top of a SiO$_2$/Si substrate and capped with a 50 nm thick SiO$_2$ protecting layer.

Two DWs, one HH and the other TT, are initially placed in the left upper and right bottom corners by applying an external field H$_0$ along the diagonal [upper image in Fig. 2(b)]. Subsequently the DWs are displaced back and forth along the upper and lower segments of the ring by applying a horizontal field H, as shown by micromagnetic simulations and magnetic force microscopy (MFM) images in Fig. 2(b). An array of structures, prepared in the initial state with the
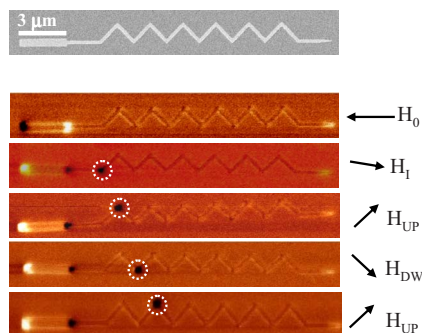
FIG. 3. (Color online) Upper panel: SEM image of the zig-zag wire structure made of Py used to implement a controllable magnetic DW step motor. Lower panel: sequence of MFM images showing the injection and propagation of a DW (marked with a dotted circle) under the action of external magnetic fields H_{UP} and H_{DW} directed as sketched in the figure.

DWs placed in the upper left and bottom right corners, is then covered with a solution containing magnetic beads (Nanomag®-D, 500 nm diameter) with a concentration of 10^6 particles/μl, until some of the beads are captured by the DWs. The diameter of the particles was chosen to enable us to monitor, in real time, the beads displacement using optical microscopy. The left-hand side of the optical microscopy image in Fig. 2(c) shows the initial state with a 2 μm cluster of magnetic nanoparticles captured by the HH DW in the upper left corner of two rings. When the horizontal external field H moves the DW from one corner to the other the particles also move to produce the configuration shown in the right-hand side of Fig. 2(c), demonstrating that the magnetic nanoparticles follow the DW motion. While the time scale of DW motion in Py wires is very short, of the order of a nanosecond over a length of a few microns,[4,6,7] in our experiment the displacement of the magnetic nanoparticles is much slower. With the time resolution of the camera we employed, we can estimate that the nanoparticle displacement takes place in a few hundreds of milliseconds. In this sense the nanoparticles do not strictly move *with* the DW but rather diffuse toward the potential energy minimum generated at the new position occupied by the DW after the application of H.

The DW displacement principle described for the square rings can be implemented in DW conduits made using nanowires structures in order to displace magnetic nanoparticles over, in principle unlimited, larger distances. The zig-zag wire structure shown in the SEM image displayed in Fig. 3, which implements a controllable magnetic DW step motor, is such an example. As for the square rings, the structure is a 30 nm thick Py wire e-beam lithographically patterned on top of a SiO_2/Si substrate and capped with a SiO_2 protecting layer 50 nm thick. The width of the wire is 200 nm while the width of the injection pad is 600 nm. Figure 3 shows also a sequence of MFM images of the injection and propagation of a DW under the action of external magnetic field pulses directed as sketched in the figure. The structure is prepared in a fully saturated initial state [configuration (1) in the MFM image sequence in Fig. 3] by applying a saturating field H_0 of 500 Oe as indicated in the figure (note: the dark and bright portions on the left and right of the injection pad are not DWs, but they are only due to the stray field at the ends of
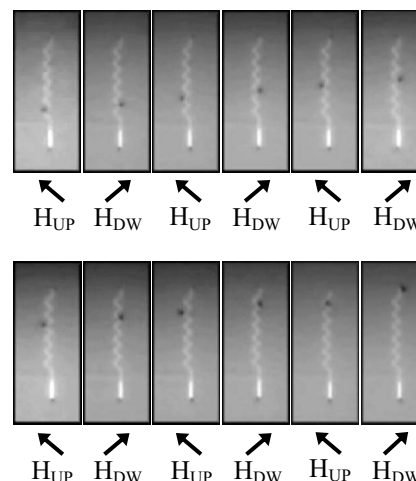

FIG. 4. Sequence of optical microscopy images of the transport of a single magnetic particle along the strip. The zig-zag is prepared in the initial state with a head-to-head DW placed in the first corner of the zig-zag conduit (configuration 3 in Fig. 3). A solution of NH_4–OH (pH=8) containing magnetic nanoparticles is dispensed on top of the chip until some of the nanoparticles are captured by the DW. Then pulsed magnetic fields with duration of 100 μs are applied to move the beads under the objective of an optical microscope.

the pad itself). Subsequently the nucleation pad is used for the nucleation of a reversed domain by applying a magnetic field H_i of 100 Oe as sketched in Fig. 3. A reversed domain nucleates in the pad at lower fields than elsewhere because the nucleation energy is lower due to its larger width and hence lower shape anisotropy than for the wire. The same magnetic field H_i causes a HH DW to propagate to the first bend in the zig-zag conduit (configuration 2 in Fig. 3). The H_i field is then removed and a sequence of fields H_{UP} and H_{DW} of 150 Oe, parallel to the wires branches are applied in order to displace the DW along each rectilinear segment and, thus, throughout the entire conduit (sequence of configurations 3–5 in Fig. 3). In order to employ this structure for bead manipulation it is then prepared in the initial state with a HH DW placed in the first corner of the zig-zag conduit (configuration 2 in Fig. 3) and the same solution, containing magnetic beads used for the previous experiment with the square rings, is dispensed on top of the structure, until one of the beads is captured by the DW. Figure 4 shows a sequence of frames of an optical microscopy video showing the transport of a single magnetic particle along the conduit obtained applying a sequence of H_{UP} and H_{DW} fields as sketched in the figure. The motion direction can be reversed at any time by reversing the direction of H_{UP} and H_{DW} in the sequence. In addition, it is worth noticing that the corners are stable position for the DW so that a magnetic nanoparticle can, if required, be held in a selected position indefinitely.

In the two cases considered so far, the actual displacement between the stable DW positions occurs through a DW motion during which neither the DW structure nor the DW speed can be completely controlled. In this sense the motion takes place step by step, each step corresponding to the distance between neighboring pinning sites for DWs, and a continuous control of the motion is not allowed. Continuous control of the nanoparticle displacement at the nanoscale,
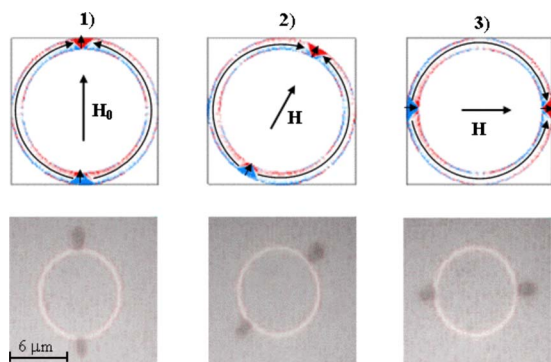
FIG. 5. (Color online) Top panel: micromagnetic simulations of the nucleation and displacement of head-to-head and tail-to-tail DWs in a circular ring obtained by applying a rotating field H. Bottom panel: optical microscopy images of the continuous displacement of two magnetic particles captured by the two DWs in a 10 μm diameter Py ring by applying a rotating field H of 300 Oe.

synchronous to that of the coupled DW, can be achieved using curved nanostrip structures, as illustrated in the next example for a circular Py ring. As in the case of the square ring, two DWs, one HH, and the other TT are spontaneously generated in a circular ring by applying a strong (saturating) magnetic field H_0. As shown by the OOMMF micromagnetic simulations of Fig. 5 (configuration 1) the DWs form upon removal of the field and lie along the direction where the field was applied. As shown in the other upper panels of Fig. 5, once created, the DWs can be moved around the circumference by the application of a smaller field H. The required magnitude is determined by the ring radius and the local DW pinning sites due to edge irregularities and material inhomogeneities as discussed below. By rotating the field both the DWs are displaced with the same angular speed as that of the rotating field, thus achieving smooth and fully controllable DW motion. Also in the present case the attractive force emanating from the DW causes the magnetic particles follow the DW as shown by the sequence of optical microscopy images in the lower panel of Fig. 5. The images show a Py circular rings of 10 μm diameter (thickness and width of 30 and 200 nm, respectively) where magnetic nanoparticles, captured by the HH and TT DWs, are displaced along the perimeter of the ring by a rotating field H of 300 Oe. By studying the motion of particles after rotation of the field by steps of 1° we verified that this geometry allows for the control of the displacement and positioning of a magnetic nanoparticle with a precision of 100 nm, as expected considering that the DW width is, in this case, about 100 nm.

The release of the magnetic particle requires the annihilation of the DW coupled to the magnetic nanoparticle. For zig-zag chains this can be achieved simply by tapering the end of the conduit thus producing weaker stray fields compared to a DW.

The concept presented here can be applied to more complex DW conduit network structures that exploit the possibility of duplicating a DW using a fan-out junction, making two split-up copies of the injected DW propagate in the two separate branches of the structure or the property that a DW traveling along a conduit can cross another conduit without being substantially modified. In this way multichannel de-

vices involving the motion of multiple DWs can be designed. The fabrication of conduits perpendicular to the plane would also allow for the creation of true 3D networks opening the way to devices with different layers of networks. Moreover, DW conduits structures can be devised to enable the simultaneous motion of multiple DWs to move several magnetic particles along the same transport line.

Another peculiarity of our approach is that one or more sensors of DWs and magnetic particles described in a previous work[18,22] can be fully integrated in a DW conduit as it essentially consists in a portion of the DW conduit, e.g., a corner, flanked by conductive contacts for detecting electrically the presence of a DW thanks to the anisotropic magnetoresistance effect. As shown in Refs. 18 and 22, the presence of a magnetic particle coupled to a DW is detected via the induced change in the magnetic field required for the displacement of the DW. Such a sensor could then be placed in the middle of a conduit and act as a magnetic particle counter, allowing for a digital control of the beads flowing on the conduits. This capability is unique compared to other technologies and pave the way to the realization of networks of conduits with externally programmable functions and continuous control of the desired process.

In conclusion we demonstrated a novel method for manipulating individual magnetic nanoparticles in suspension thanks to the interaction between them and DWs propagating in magnetic nanostrips. The method allows for the capture, transport, and release of particles in lab-on-chip devices, with control of their position at the nanometer scale, simply by application of external magnetic fields.

In perspective, the approach described here may support and integrate single molecule manipulation on chip with a much lower degree of complexity compared to the tools developed so far, which are highly sophisticated, require accurate calibration, and are not suitable to be implemented in lab-on-chip devices.[23]

[1]R. D. McMichael and M. J. Donahue, IEEE Trans. Magn. **33**, 4167 (1997).
[2]Y. Nakatani, A. Thiaville, and J. Miltat, Nature Mater. **2**, 521 (2003).
[3]S. S. P. Parkin, M. Hayashi, and L. Thomas, Science **320**, 190 (2008).
[4]T. Ono, H. Miyajima, K. Shigeto, K. Mibu, N. Hosoito, and T. Shinjo, Science **284**, 468 (1999).
[5]D. A. Allwood, G. Xiong, M. D. Cooke, C. C. Faulkner, D. Atkinson, N. Vernier, and R. P. Cowburn, Science **296**, 2003 (2002).
[6]D. Atkinson, D. A. Allwood, G. Xiong, M. D. Cooke, and R. P. Cowburn, Nature Mater. **2**, 85 (2003).
[7]G. S. D. Beach, C. Nistor, C. Knutson, M. Tsoi, and J. L. Erskine, Nature Mater. **4**, 741 (2005).
[8]A. Yamaguchi, T. Ono, S. Nasu, K. Miyake, K. Mibu, and T. Shinjo, Phys. Rev. Lett. **92**, 077205 (2004).
[9]M. Kläui, C. A. F. Vaz, J. A. C. Bland, W. Wernsdorfer, G. Faini, E. Cambril, L. J. Heyderman, F. Nolting, and U. Rüdiger, Phys. Rev. Lett. **94**,

106601 (2005).

[10] P. Vavassori, V. Metlushko, and B. Ilic, Appl. Phys. Lett. **91**, 093114 (2007).

[11] D. A. Allwood, G. Xiong, C. C. Faulkner, D. Atkinson, D. Petit, and R. P. Cowburn, Science **309**, 1688 (2005).

[12] T. Deng, G. M. Whitesides, M. Radhakrishnan, G. Zabow, and M. Prentiss, Appl. Phys. Lett. **78**, 1775 (2001).

[13] C. S. Lee, H. Lee, and R. M. Westervelt, Appl. Phys. Lett. **79**, 3308 (2001).

[14] A. H. B. De Vries, B. E. Krenny, R. van Driel, and J. S. Kanger, Biophys. J. **88**, 2137 (2005).

[15] K. Gunnarsson, P. E. Roy, S. Felton, J. Pihl, P. Svedlindh, S. Berner, H. Lidbaum, and S. Oscarsson, Adv. Mater. (Weinheim, Ger.) **17**, 1730 (2005).

[16] R. S. Conroy, G. Zabow, J. Moreland, and A. P. Koretsky, Appl. Phys. Lett. **93**, 203901 (2008).

[17] M. J. Donahue and D. G. Porter, *OOMMF User's Guide, Version 1.0.*

Interagency Report NISTIR 6376 (National Institute of Standards and Technology, Gaithersburg, 1999).

[18] P. Vavassori, V. Metlushko, B. Ilic, M. Gobbi, M. Dolonato, M. Cantoni, and R. Bertacco, Appl. Phys. Lett. **93**, 203502 (2008); R. Bertacco and P. Vavassori, European Patent Application No. PCT/EP2009/054808, 2009.

[19] L. E. Helseth, T. M. Fischer, and T. H. Johansen, Phys. Rev. Lett. **91**, 208302 (2003).

[20] L. E. Helseth, T. M. Fischer, and T. H. Johansen, Phys. Rev. E **67**, 042401 (2003).

[21] P. Vavassori, M. Grimsditch, V. Novosad, V. Metlushko, and B. Ilic, Phys. Rev. B **67**, 134429 (2003); A. Libál, M. Grimsditch, V. Metlushko, P. Vavassori, and B. Jankó, J. Appl. Phys. **98**, 083904 (2005).

[22] M. Donolato, M. Gobbi, P. Vavassori, M. Leone, M. Cantoni, V. Metlushko, B. Ilic, M. Zhang, S. X. Wang, and R. Bertacco, Nanotechnology **20**, 385501 (2009).

[23] K. C. Neuman and A. Nagy, Nat. Methods **5**, 491 (2008).